

CHAPTER 60

Shoaling and Reflection of Nonlinear Shallow Water Waves

Padmaraj Vengayil¹ and James T. Kirby²

The formulation for shallow water wave shoaling and refraction-diffraction given by Liu *et al* (1985) is extended to include reflected waves. The model is given in the form of coupled K-P equations for forward and backward propagation. Shoaling on a plane beach is studied using the forward-propagating model alone. Non-resonant reflection of a solitary wave from a slope and resonant reflection of periodic waves by sinusoidal bars are then studied.

Introduction

Recently, Liu *et al* (1985) have developed a set of coupled parabolic equations to study the combined refraction and diffraction of time-periodic waves in shallow water over two-dimensional topography. Derivations in that study were based both on the Boussinesq equations for variable depth (Peregrine, 1972) and a variable depth form of the equation of Kadomtsev and Petviashvili (1970) (K-P), leading to similar results. The resulting equations model only the incident wave and neglect the reflected wave component. The problem of the neglected reflected wave component is important, both to the prediction of shoaled wave heights over gentle slopes and to the prediction of waves propagated over undular nearshore topography, which can lead to significant reflection by means of a resonance mechanism.

In this study, we address several questions of accuracy of predictions of the forward-scattered parabolic approximation which were not addressed in the previous study. In particular, we study the shoaling of a normally incident wave on a plane beach and analyze results both in terms of wave-height and wave form prediction in comparison with laboratory data. We then formulate coupled equations for incident and reflected waves and study wave reflection in several situations.

Model Formulation

Following a usual procedure for obtaining coupled parabolic equations for strictly monochromatic waves, we instead study the linear

¹Graduate Student, Coastal and Oceanographic Engineering Department, University of Florida, Gainesville, FL (presently, Department of Civil Engineering, Massachusetts Institute of Technology, Cambridge, MA)

²Assistant Professor, Coastal and Oceanographic Engineering Department University of Florida, Gainesville, FL

nondispersive wave equation for arbitrary surface displacement $\eta(x,y,t)$. Letting $\eta = \eta^+ + \eta^-$, with $\eta^{+(-)}$ denoting forward (backward) propagating components of the wave field (with respect to direction x), we obtain a set of equations which are coupled through the local bottom variations. The equations are extended to include weakly dispersive and weakly nonlinear effects, yielding model equations of the form

$$\frac{1}{c} \eta_t^+ + \eta_x^+ + \frac{h}{4h} (\eta^+ - \eta^-) + \frac{3}{2h} \eta^+ \eta_x^+ + \frac{h^2}{6} \eta_{xxx}^+ - \int_x^\infty \frac{1}{2h} (h\eta_y^+)_y dx = 0 \quad (1a)$$

$$\frac{1}{c} \eta_t^- - \eta_x^- + \frac{h}{4h} (\eta^+ - \eta^-) - \frac{3}{2h} \eta^- \eta_x^- - \frac{h^2}{6} \eta_{xxx}^- + \int_x^\infty \frac{1}{2h} (h\eta_y^-)_y dx = 0 \quad (1b)$$

where $h(x,y)$ is the local water depth and $c(x,y) = (gh)^{1/2}$. We subsequently neglect y -variations and study x -direction propagation alone for the remainder of this study. Details of the derivation may be found in the report by Vengayil and Kirby (1986). For the case of time-aperiodic motions, equations (1) are altered to RLW form and solved conveniently using a variation of the three time level scheme of Eilbeck and McGuire (1977). For the case of wave forms η^+ , η^- which vanish as $|x| \rightarrow \infty$, it is further possible to show that equations (1) lead to the mass conservation law

$$\frac{d}{dt} \int_{x_0}^\infty (\eta^\pm) dx = \pm \tilde{Q}^\pm \pm \int_{x_0}^\infty c_x \eta dx \quad (2)$$

where x_0 is some arbitrary station and

$$\tilde{Q}^\pm(x_0) = \left\{ c\eta^\pm + \frac{3c\eta^{\pm 2}}{4h} + \frac{ch^2}{6} \eta_{xx}^\pm \right\} \Big|_{x_0} \quad (3)$$

represents the flux of mass across station x_0 . Taking the limit $x_0 \rightarrow -\infty$ then gives

$$\frac{d}{dt} \int_{-\infty}^\infty \eta^+ dx = - \frac{d}{dt} \int_{-\infty}^\infty \eta^- dx = \int_{-\infty}^\infty c_x \eta dx$$

or

$$\int_{-\infty}^\infty \eta dx = \text{constant} \quad (4)$$

indicating exact mass conservation. For the case of weak reflection with $O(|\eta^-|) \sim O(h_x) \cdot O(|\eta^+|)$, the source (sink) term is altered to

$$\int_{-\infty}^{\infty} c_x \eta dx = \int_{-\infty}^{\infty} c_x \eta^+ dx + O(|c_x|^2) \quad (5)$$

and the conclusions on mass balance in the variable coefficient KdV equation given by Miles (1979) are recovered.

For the case of time-periodic motions, the surface displacements η^+ , η^- may be expanded in Fourier series with slowly-varying modal amplitudes; we then solve the coupled O.D.E. evolution equations for the amplitudes.

Shoaling of Regular Waves

We first study the shoaling of a regular wave on a plane beach as a means of further testing the accuracy of the model developed by Liu *et al* (1985). Data for the height and wave-form of shoaling waves were obtained from the results presented by Buhr Hansen and Svendsen (1979) and further described by Svendsen and Buhr Hansen (1978) and Buhr Hansen (1980). Figure 1 shows the configuration of the wave flume used in the tests. The five longest wave conditions were chosen for study; parameters for the chosen tests are shown in Table 1.

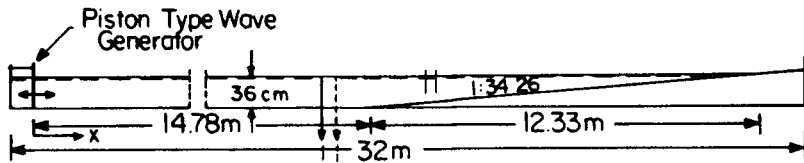


Figure 1. Experimental set-up of Buhr Hansen and Svendsen (1979).

Table 1 Wave parameters at the wavemaker for the test considered from Buhr Hansen and Svendsen (1979).

Buhr Hansen & Svendsen Test No.	H_0 (m) (actual)	$\epsilon = \frac{H_0}{2h_0}$	T(sec)	$\mu^2 = \frac{\omega^2 h_0}{g}$	U_{r0}
051071	0.067	0.090	2.0	0.362	0.248
051041	0.037	0.051	2.0	0.362	0.140
041071	0.070	0.097	2.5	0.232	0.418
041041	0.040	0.056	2.5	0.232	0.242
031041	0.040	0.056	3.33	0.130	0.445

The model equations were developed by neglecting the wave reflected from the slope, which has been shown to be small (Vengayil and Kirby, 1986). The incident wave η^+ is represented by the Fourier series

$$\eta^+(x,t) = \sum_{n=1}^N A_n(x) e^{in(\int k dx - \omega t)} + c.c. \quad ; \quad \omega = ck \quad (6)$$

The series is substituted in equation (1a) (neglecting η^-) to give

$$A_{n_x} + \frac{h_x}{4h} A_n - \frac{in^3 k(kh)^2}{12} A_n + \frac{3ink}{8h} \left\{ \sum_{\ell=1}^{n-1} A_\ell A_{n-\ell} + 2 \sum_{\ell=1}^{N-n} A_\ell A_{n+\ell} \right\} = 0$$

n=1, ..., N (7)

The model equation may be extended to include laminar frictional damping due to bottom and sidewalls by the addition of the term

$$\frac{(1+i)}{2h} n^2 k^2 \left(\frac{2\nu}{nw}\right)^{1/2} \left\{1 + \frac{2h}{b}\right\} A_n \quad (8)$$

to equation (7). Here, ν is the kinematic viscosity and b is the channel width.

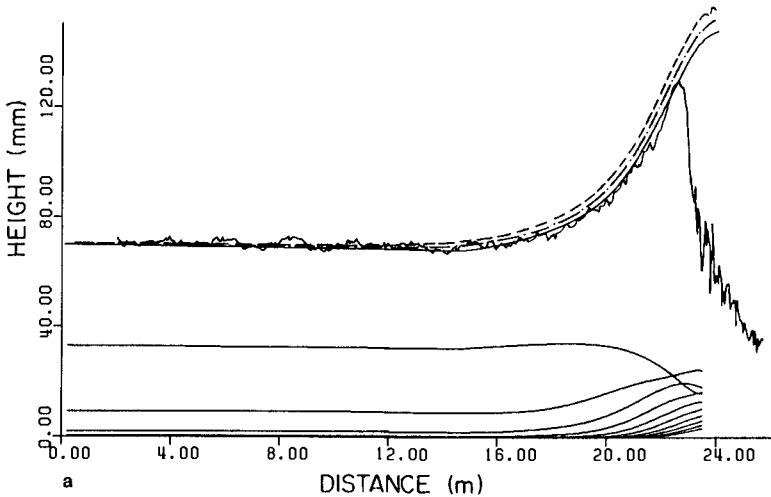
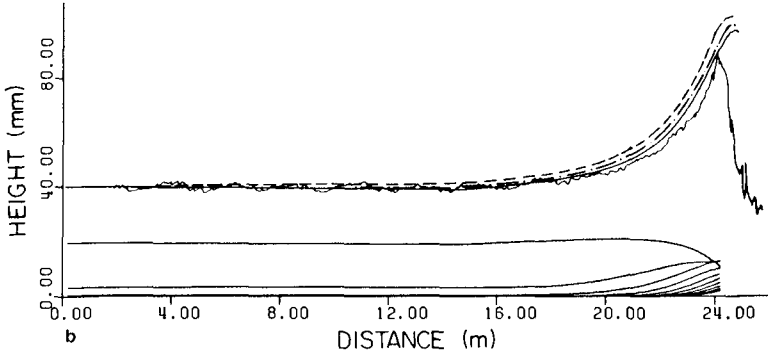
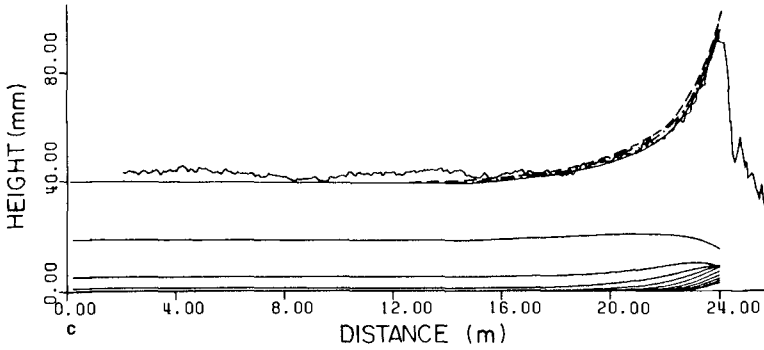


Figure 2. a) TEST 041071, T = 2.5 sec, H = 0.07 m.



b) TEST 041041, T = 2.5 sec, H = 0.04 m.



c) TEST 031041, T = 3.33 sec, H = 0.04 m.

Figure 2. Numerical results of shoaled wave height, (----, inviscid theory; -·-·-, bottom friction included —, bottom and side wall friction included) compared to experimental results of Buhr Hansen and Svendsen (1979). Also shown are the component amplitudes $|A_1| - |A_{10}|$ for flow with bottom and side wall friction.

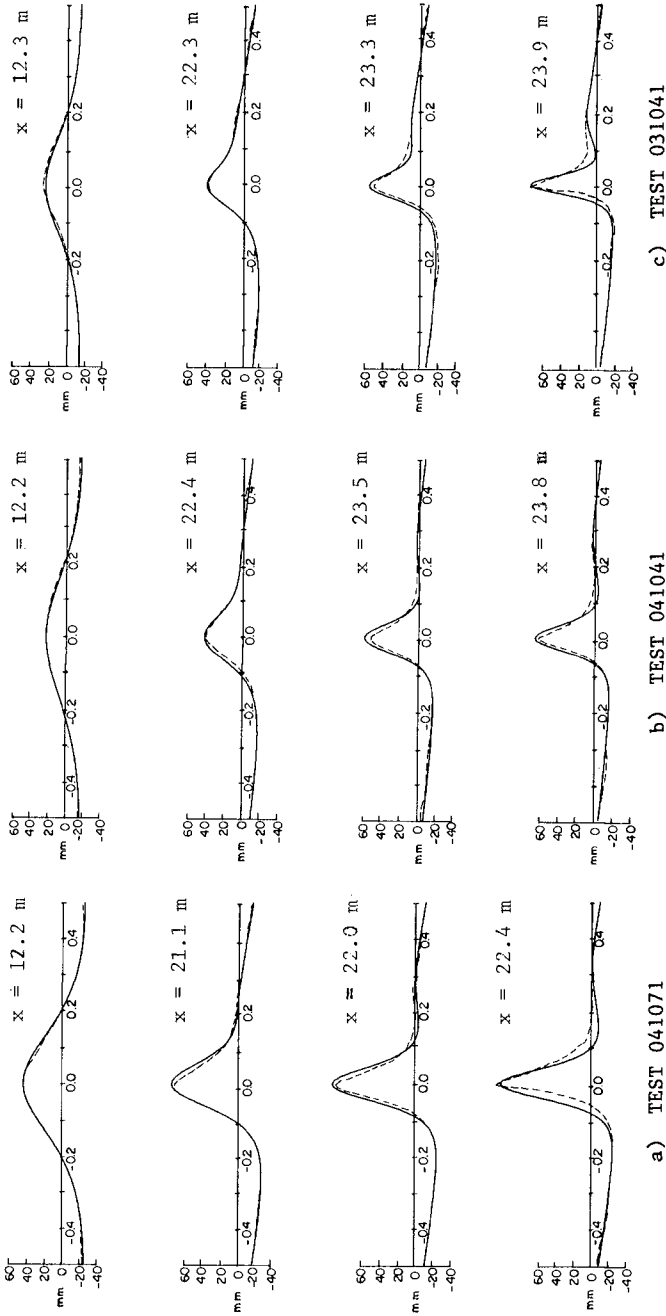


Figure 3. Comparison of wave profiles predicted by the numerical model including bottom and side wall friction effects with the experimental results of Buhr Hansen and Svendsen (1979).
 — numerical, - - - experimental. Distances are from wavemaker in Figure 1.

Results for shoaled wave heights are shown in Figure 2a-c for the three longest waves studied. Results are shown for undamped waves, damping due to bottom friction alone, and damping due to bottom and sidewalls. Also included are plots of component amplitudes $|A_1| - |A_{10}|$ for the case with sidewall damping. The reproduction of shoaling wave height is good for the damped cases.

Figure 3 shows computed wave forms in comparison to experimentally measured waves for the cases with bottom and sidewall damping. Reproduction of measured wave form is quite good except in regions close to wave breaking. In these regions the forward face of the wave tilts towards a vertical position and vertical accelerations become quite large, thus invalidating the Boussinesq approximation locally. However, the model has no apparent difficulty in predicting shoaled wave height up to the breaking limit. An investigation of the higher order skewness and asymmetry properties of the shoaled waves is presently underway and will be reported subsequently.

Gradual Reflection of Solitary Waves

A test of the coupled equations was performed by comparing results for reflection of a solitary wave by an underwater slope with experimental data obtained by Goring (1978). Goring also computed theoretical results for reflection coefficients based on numerical

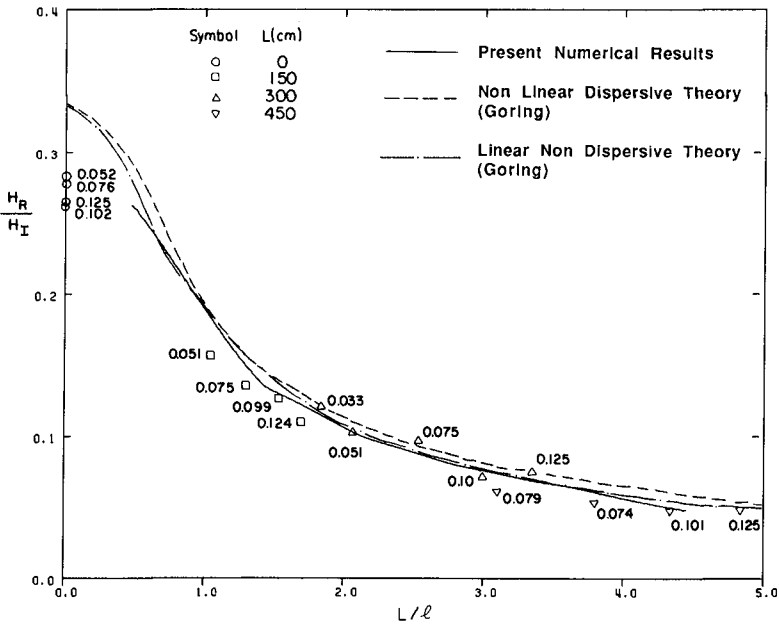


Figure 4. Reflection coefficients for solitary waves propagating over a submerged slope. Data from Goring (1978).

solution of the Boussinesq equations (weakly nonlinear-weakly dispersive case) and on the Bessel function solution of the linear-nondispersive shallow water equation. Figure 4 gives results of reflection coefficient based on the ratio of height of reflected wave to height of incident wave for varying values of slope length L to incident wavelength ℓ , for a particular case of a depth reduction $h_1/h_2 = 4$. The incident wave length is estimated here according to

$$\ell = 1.5 (H_I/h_1)^{-1/2} h_1 \quad (9)$$

Results of the present study agree most closely with the linear nondispersive theory, indicating the overall dominance of the slope effect in the scattering process. The present theory and Goring's linear theory each deviate slightly from Goring's nonlinear theory, indicating that there is some effect due to nonlinear coupling between the incident and reflected wave. This discrepancy is presently being investigated using a version of the present theory which retains nonlinear coupling between the opposite-going waves.

An example of the time history of a solitary wave reflection for a particular case of a fairly abrupt slope is given in Figure 5. The development of the reflected wave, moving to the left with increasing time, is apparent, as is the nonlinear evolution of the incident wave after it moves onto the shelf. This evolution involves the generation of three soliton modes which are rank-ordered in height and subsequently disperse due to the nonlinear evolution. The reflected wave is seen to have about the same width as the incident wave (as would be expected for a short slope) and evolves only slowly due to its low initial amplitude (scale on right). The presence of a high frequency tail following each wave train is just becoming apparent on the top trace of the picture.

Resonant Reflection by Sand Bars

Recently, Mei (1985) has investigated the resonant interaction which occurs between an incident wave of wavenumber k , a synchronous reflected wave with wavenumber $-k$ and a bar field with dominant wavenumber $\lambda = 2k$. Mei's investigation was for the case of linearized, intermediate depth theory. Here, we have extended the investigation to the case of nonlinear, weakly-dispersive waves. The topography studied had the form

$$h(x) = \begin{cases} h_0 & x < 0 ; x > L \\ h_0 + D \sin \lambda x & 0 < x < L \end{cases} \quad (10)$$

where D is the bar amplitude and $\lambda = 2\pi/\ell_b$ is the bar wavenumber. Results are presented here for $L = 4\ell_b$ (four bars in the patch). The relevant governing equations are developed by using equation (6) for the incident wave η^+ and

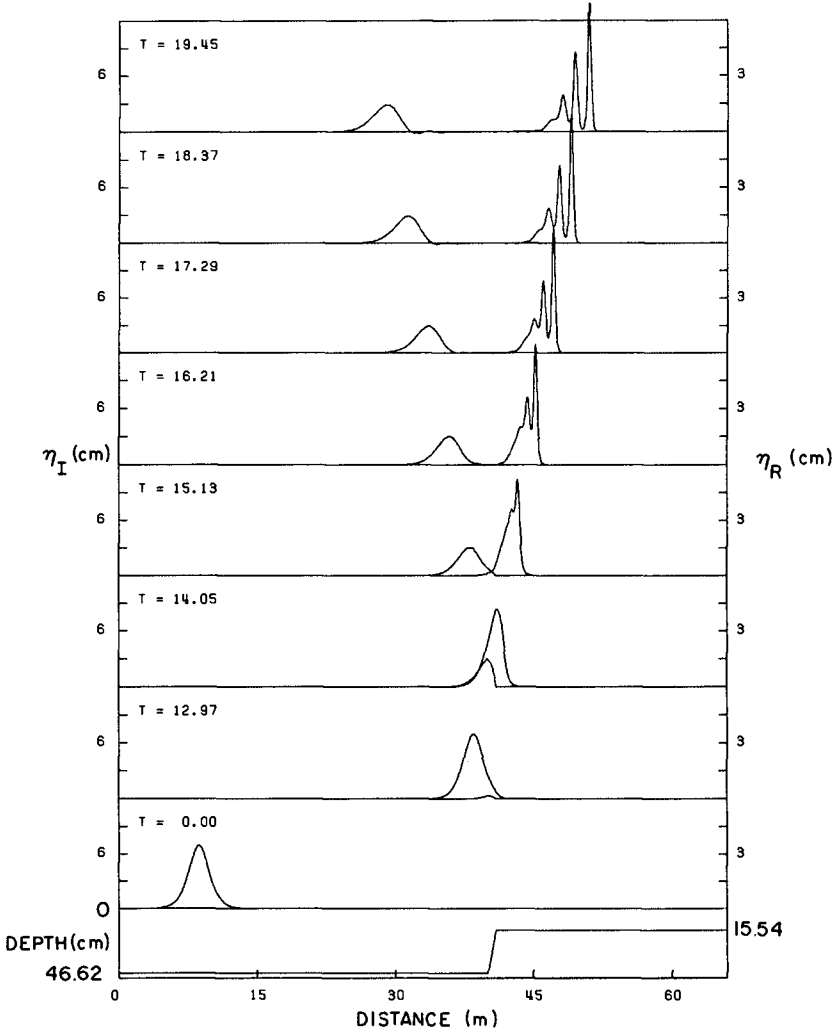


Figure 5. Evolution of a solitary wave. Incident wave propagates to the right.

$$\eta^-(x,t) = \sum_{n=1}^N B_n(x) e^{-in(\int k dx - \omega t)} + c.c. \quad (11)$$

for the reflected wave. Substitution of (6) and (11) in the governing model equation (1) leads to the coupled system of evolution equations

$$A_{n_x} + \frac{h_x}{4h} (A_n - B_n e^{-2in\int k dx}) - \frac{in^3 k^3 h^2}{12} A_n + \frac{3ink}{8h} \left[\sum_{\ell=1}^{n-1} A_\ell A_{n-\ell} + 2 \sum_{\ell=1}^{N-n} A_\ell^* A_{n+\ell} \right] = 0 \quad (12)$$

and

$$B_{n_x} + \frac{h_x}{4h} (B_n - A_n e^{2in\int k dx}) + \frac{in^3 k^3 h^2}{12} B_n - \frac{3ink}{8h} \left[\sum_{\ell=1}^{n-1} B_\ell B_{n-\ell} + 2 \sum_{\ell=1}^{N-n} B_\ell^* B_{n+\ell} \right] = 0 \quad (13)$$

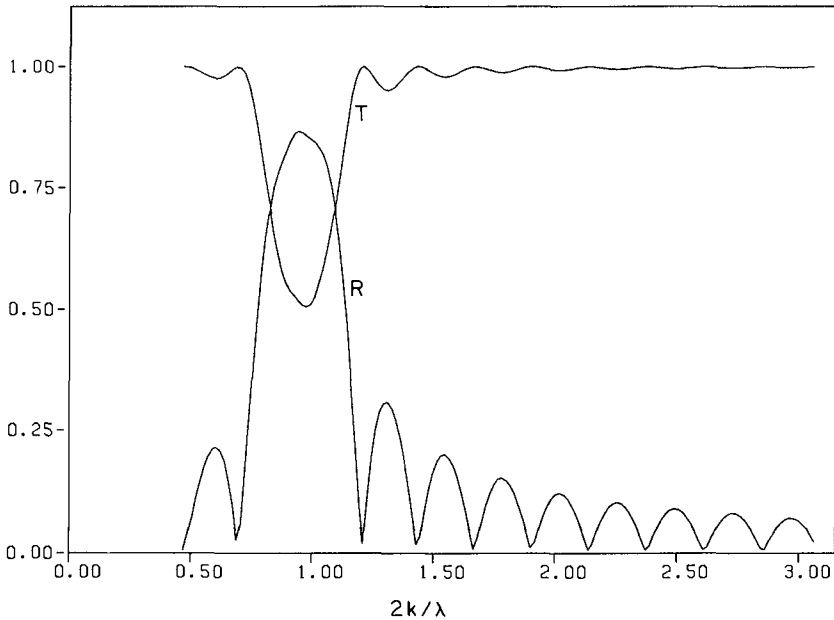


Figure 6. a) linear theory

The incident wave $A_n(0)$ is specified according to a spectral solution for permanent waves in the RLW equation (Vengayil and Kirby, 1986). The $B_n(L)$ are set equal to zero, representing the case of no waves arriving at the patch from large positive x .

Figure 6 shows results for $D/h_0 = 0.4$ and $n=4$ for a range of bar lengths relative to a fixed wavelength. The plots give calculated reflection coefficient $R_1 = |B_1(0)/A_1(0)|$ and transmission coefficient $T_1 = |A_1(L)/A_1(0)|$ as solid lines. This represents the complete solution for linear theory (Figure 6a). The presence of the resonant peak at $2k/\lambda = 1$ is apparent. In Figure 6b (nonlinear theory), the results for the reflection coefficient R_1 , which now represents only one component of the wave field, does not differ greatly from the linear result. This result may be of some importance since it indicates that the linear scattering process dominates the nonlinear effects over the relatively short bar field, which would allow the application of the linear scattering theory in a nearshore, nonlinear wave field.

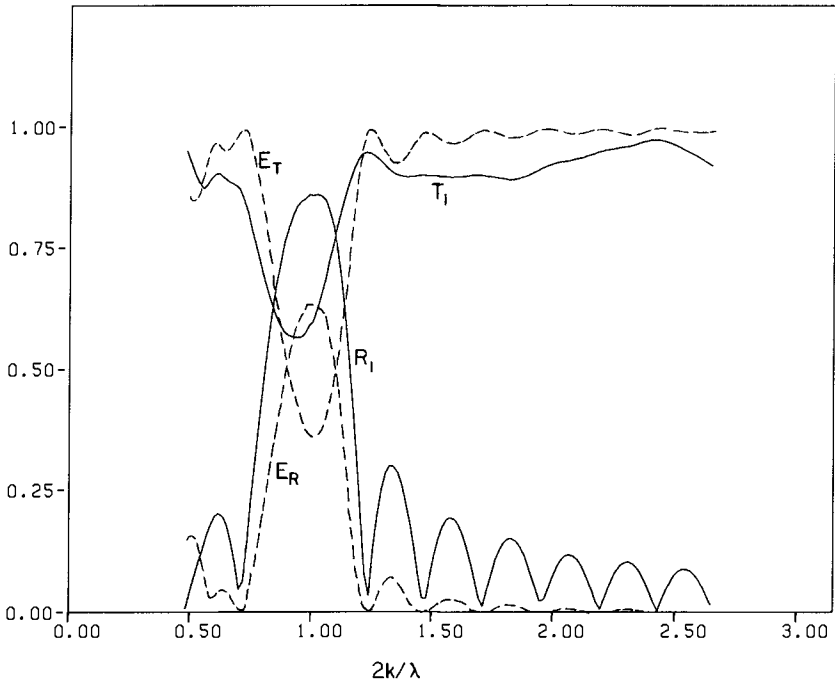


Figure 6. Reflection and transmission of waves by a sinusoidal bar patch. $n=4$, $D/h = 0.4$.
b) nonlinear theory.

Also shown in Figure 6b are traces of the total transmitted energy E_T and reflected energy E_R normalized by the total incident energy. The numerical scheme was found to satisfy the requirement

$$E_R + E_T = 1 \quad (14)$$

to several decimal places for suitably fine discretizations of the physical domain. The only effect due to nonlinearity which is readily apparent in the results in Figure 6b is the drop in T_1 below one for $2k/\lambda > 1$. This effect represents a transfer of energy to higher harmonics following from destabilization of the incident wave during its shoaling over the bar crests.

Finally, Figure 7 shows the evolution of the spectral amplitude components during nonlinear evolution at the resonant condition in Figure 6. Only the growth of $|B_1|$ is strongly forced by the reflection process; the growth of $|B_2|$ and $|B_3|$ may be partially due to reflection but also is influenced strongly by the nonlinear transfer of energy from $|B_1|$ as it grows. Likewise, $|A_1|$ may gain energy from its harmonics as the incident wave loses energy over the bar field, which would tend to increase the apparent reflection. These two nonlinear effects thus compete in the overall reflection process, and their possible near-cancellation may contribute to the relatively small change in reflection coefficients noted in shifting from linear to nonlinear theory. This effect is presently being investigated in the context of resonantly-reflected solitary waves.

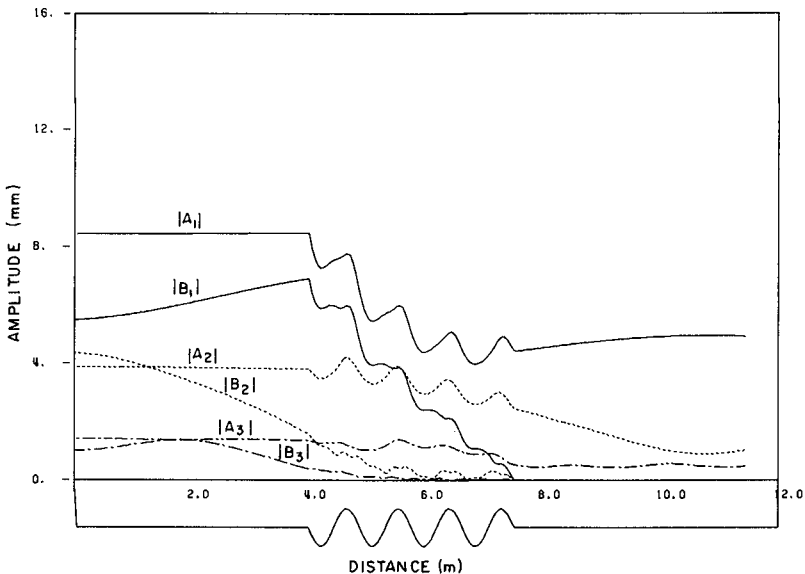


Figure 7. Evolution of component amplitudes $|A_1|$ - $|A_3|$ and $|B_1|$ - $|B_3|$ for the resonant peak of Figure 6. Nonlinear theory.

References

- Buhr Hansen, J., 1980, "Experimental investigations of periodic waves near breaking", Proc. 17th Intl. Conf. Coast. Eng., ASCE, 260-277.
- Buhr Hansen, J. and Svendsen, I.A., 1979, "Regular waves in shoaling water, experimental data", Series paper 21, Institute Hydro. and Hydraulic Eng., Tech. Univ. Denmark.
- Eilbeck, J.C. and McGuire, G.R., 1977, "Numerical study of the regularized long wave equation 1: numerical methods", J. Comp. Phys. 19, 43-57.
- Freilich, M.H. and Guza, R.T., 1984, "Nonlinear effects on shoaling surface gravity waves", Phil. Trans. Roy. Soc. A311, 1-41.
- Goring, D.G., 1978, "Tsunamis - the propagation of long waves onto a shelf", Report KH-R-38, W.M. Keck Lab. Hydr. and Water Res., California Inst. Tech., Pasadena.
- Kadomtsev, B.B. and Petviashvili, V.I., 1970, "On the stability of solitary waves in weakly dispersive media", Sov. Phys. Dokl. 15, 539-541.
- Liu, P.L.-F., Yoon, S.B. and Kirby, J.T., 1985, "Nonlinear refraction-diffraction of waves in shallow water", J. Fluid Mech. 153, 185-201.
- Mei, C.C., 1985, "Resonant reflection of surface water waves by periodic sand bars", J. Fluid Mech. 152, 315-335.
- Miles, J.W., 1979, "On the Korteweg-deVries equation for a gradually varying channel", J. Fluid Mech., 91, 181-190.
- Peregrine, D.H., 1972, "Equations for water waves and the approximations behind them", in Waves on Beaches R.E. Meyer (ed.), Academic Press, 95-121.
- Svendsen, I.A. and Buhr Hansen, J., 1978, "On the deformation of periodic long waves over a gently sloping bottom", J. Fluid Mech. 87, 433-448.
- Vengayil, P. and Kirby, J.T., 1986, "Shoaling and reflection of nonlinear shallow water waves", Tech. Rept. UFL/COEL-TR/062, Coastal and Oceanographic Eng. Dept., Univ. of Florida, Gainesville.